ON THE FINITE-STATE MODELING AND OBSERVABILTY OF AEROSERVOELASTIC SYSTEMS

Mastroddi, F., De Troia, R.
Dipartimento Aerospaziale - Università degli Studi di Roma "La Sapienza"
Via Eudossiana 18, 00184 Rome, Italy

Morino, L.,
Dipartimento di Meccanica ed Automatica - Terza Università degli Studi di Roma
Via Ostiense 159, 00154 Rome, Italy

Pecora M.
ALENIA, Pomigliano d'Arco, Italy

Abstract Within a linear formulation (in particular, potential subsonic or supersonic flows) - using a boundary element method for the aerodynamics, a modal approach for the structural dynamics, and optimal control theory for active control - we introduce a recently developed least-square procedure for the finite-state approximation of the aerodynamic matrix in order to reduce the aeroservoelastic system to the stardard state space form $\dot{\mathbf{x}} = \mathbf{A}\mathbf{x} + \mathbf{B}\mathbf{u}$, $\mathbf{y} = \mathbf{C}\mathbf{x}$. The state-space vector $\mathbf{x}$ includes certain aerodynamic states introduced in the modeling process which cannot be measured in order to control the system. The advantages of the approach and some issues related with the use of a reduced-order observer of the state for the control of the system are discussed. In particular, if the finite-state aerodynamic model introduced is stable, the reduced-order observer used for estimating the state of the system can have a dynamics closely related to that of the aerodynamic portion of the state-space vector. Numerical results on assessment of the model accuracy and on the pratical use of the reduced-order observer for a 3D system are included.

Introduction

The objective of this paper is to present some applications of a recently developed finite-state aerodynamic model. In particular, we show how one may develop a simple reduced-order observer for the aerodynamic portion of the state vector under the assumption that (1) the complete structural dynamics portion of the state vector may be obtained from the output and (2) the matrix of the aerodynamics portion of the model (see matrix $\mathbf{A}_{22}$, Eq. 23) is stable.

In order to clarify the above issue, in the following we introduce some basic concepts on aeroservoelastic model in terms of state-space variables and finite-state aerodynamics. Consider an aeroelastic system described in terms of the amplitudes, $q_n(t)$, of the natural modes of vibration, ϕ_n, which are here assumed to be normalized, so as to have the generalized masses equal one. The corresponding Lagrange equations of motion, neglecting structural damping and gravity, are given by

$$\frac{\mathrm{d}^2\mathbf{q}}{\mathrm{d}\,t^2} + \mathbf{\Omega}^2\mathbf{q} = q_D\,\mathbf{f} \tag{1}$$

where $\mathbf{\Omega}$ is the diagonal matrix of the natural frequencies of vibration of the structure, and $q_D = \varrho_\infty U_\infty^2/2$ is the dynamic pressure, whereas the components of $\mathbf{f}$ are the generalized aerodynamic forces associated with the n^{th} mode, ϕ_n $(n = 1, ..., N)$, as

$$q_D\, f_n = \iint_{\mathcal{S}} \mathbf{t} \cdot \phi_n \, d\mathcal{S} \tag{2}$$

where $\mathbf{t}$ is the aerodynamic force per unit area acting on $\mathcal{S}$.

In the following, we consider the presence of control surfaces as additive degrees of freedom. For the sake of simplicity, we consider only one control surface, corresponding to the state-space variable, q_δ. This yields a system with one control variable (single-input system). The formulation for several control surfaces (multiple-input system) is closely related.[12]

In order to take into account also the control-surface motion, a servolaw is added to the Lagrangean equations, and Eq. 1 is modified into

$$\mathbf{M}\frac{\mathrm{d}^2\mathbf{q}}{\mathrm{d}\,t^2} + \mathbf{K}\mathbf{q} = q_D\mathbf{f} + \hat{\mathbf{b}}u \tag{3}$$

with

$$\mathbf{M} := \begin{bmatrix} \mathbf{I} & \mathbf{m} \\ \mathbf{m}^{\mathrm{T}} & m_\delta \end{bmatrix} \qquad \mathbf{q} := \begin{Bmatrix} q_1 \\ \cdots \\ q_N \\ q_\delta \end{Bmatrix}$$

$$\mathbf{K} := \begin{bmatrix} \boldsymbol{\Omega}^2 & \mathbf{0} \\ \mathbf{0}^{\mathrm{T}} & m_\delta\omega_{cs}^2 \end{bmatrix} \quad \mathbf{f} := q_D\begin{Bmatrix} f_1 \\ \cdots \\ f_N \\ f_\delta \end{Bmatrix} \quad \hat{\mathbf{b}} := \begin{Bmatrix} 0 \\ \cdots \\ 0 \\ 1 \end{Bmatrix}$$

where m_δ and $m_\delta\omega_{cs}^2$ are, respectively, the moment of inertia and the hinge stiffness of the control surface, whereas $\mathbf{m}$ is the vector of the coupling generalized masses, $q_D f_\delta$ is the control-surface aerodynamic moment (linear function of $\mathbf{q}$), and u the applied control moment).

Here, we assume that the aerodynamic forces depend linearly upon the Lagrangean coordinates $q_n(t)$; specifically, in the following we limit ourselves to potential subsonic or supersonic flows (although the applications do not include supersonic flows). Hence, the Laplace transform of the generalized force vector can be expressed as*

$$\tilde{\mathbf{f}}(s) = \mathbf{E}\left(\frac{s\ell}{U_\infty}\right)\tilde{\mathbf{q}}(s) \tag{4}$$

where $\mathbf{E}$ is the so-called aerodynamic matrix. As well known and as emphasized in Eq. 4, $\mathbf{E}$ is a function of s and U_∞ only through the variable $p := s\ell/U_\infty$, which is known as the complex reduced frequency. Note that $\mathbf{E}(p)$ may be obtained analytically for some simple cases (*e.g.*, classic Theodorsen incompressible 2-D aerodynamic theory); otherwise, $\mathbf{E}(p)$ is evaluated numerically, for instance, by lifting-surface, doublet-lattice, or panel methods. Typically, the algorithm for the evaluation of $\mathbf{E}(p)$ is available only along the imaginary axis: $\mathbf{E}(p)$ is then the analytic continuation of $\mathbf{E}(ik)$, with $k = \omega\ell/U_\infty$ (reduced frequency).

Next, consider finite-state aerodynamic modeling, *i.e.*, a process whereby the aerodynamic transfer function is approximated by means of appropriate rational expressions. Probably, the earliest example of this approach is the work of Jones[1] who gives a rational approximation for the Theodorsen function and the corresponding time-domain approximation for the Wagner function. In more recent examples of this approach[2, 7], closely related techniques are used in order to obtain approximate expressions, either of the Theodorsen function, or directly of the aerodynamic matrix.

As a result, the aeroelastic model, Eq. 1, may be rewritten, in the time domain, as (see Eqs. 10 and 10)

$$\dot{\mathbf{x}} = \mathbf{A}\mathbf{x} + \mathbf{B}\mathbf{u} \tag{5}$$

with the output $\mathbf{y}$ given by (see Eq. 18)

$$\mathbf{y} = \mathbf{C}\mathbf{x} \tag{6}$$

This yields apparent advantages for the aeroelastic analysis (for instance, the V-g method may be replaced by a simple root locus) and for active control utilization (for instance, in the use of optimal control techniques). The approach used here is that of Refs. 8 and 9 and is summarized in the next section.**

Next, let us consider some issues which arises with the application of finite-state aerodynamics to aeroservoelasticity. In order to discuss this issue, let us review some basic concepts from the theory of active control. If $\mathbf{y} = \mathbf{x}$ (*i.e.*, if $\mathbf{C} = \mathbf{I}$, see Eq. 6), then, in order to accomplish a certain objective (such as, flutter suppression or gust alleviation), one may design (either by eigenvalue assignment or by optimal-control techniques) a regulator, *i.e.*, a feedback of the type

$$\mathbf{u} = -\mathbf{K}\mathbf{x} \tag{7}$$

This is still possible whenever $\mathbf{x}$ is measurable (*i.e.*, if the state vector $\mathbf{x}$ may be obtained from the output vector $\mathbf{y}$, for instance, if $\mathbf{C}$ is a nonsingular square matrix).

However, in our case, this is not true. Indeed, a basic feature of finite-state aerodynamic modeling is the introduction of additional state variables. These additional variables (corresponding to aerodynamic states) cannot be obtained from the output. Whenever the state vector is not measurable, a full-state observer (state estimator) may be used in order to obtain, from $\mathbf{y}$ and $\mathbf{u}$, an estimate, $\hat{\mathbf{x}}$, of the state variables $\mathbf{x}$.[12] Then, in designing a suitable regulator, one may use the separation principle,[12] which guarantees that one may design this regulator as if all the state variables were available, and then use the estimate $\hat{\mathbf{x}}$ (*i.e.*, the output of the estimator) as the input to the regulator. The above issues (*i.e.*, full-state observer) has been addressed, in connection with aeroservoelastic problems, by Lu and Huang[13], with applications limited to 2D problems.

In this paper, we want to take the formulation a step further, *i.e.*, we want to address the problem of the

* In this paper the Laplace transform of a time dependent function $f(t)$ is indicated as $\tilde{f}(s)$, where s is the Laplace variable.

** The approach of Refs. 8 and 9 is closely related to that developed independently by Ghiringhelli and Mantegazza[10]: whereas the basic formulations coincide, the implementations, in particular the higher-order approach, differ considerably. A synthesis of the two approach is presented in Ref. 11.

reduced-order observer. Specifically, in the case under consideration, one may use a specialized formulation, under the assumption that all the structural-dynamics variables, $\mathbf{q}$ and $\dot{\mathbf{q}}$ are available for control (indeed, this is the best one may hope for). For simplicity, we adopt here this assumption, *i.e.*, that

$$\mathbf{y} := \mathbf{C}_1 \left\{ \begin{matrix} \mathbf{q} \\ \dot{\mathbf{q}} \end{matrix} \right\} = [\mathbf{C}_1 | \mathbf{0}]\mathbf{x} \tag{8}$$

where $\mathbf{C}_1$ is a square nonsingular matrix, whereas the matrix $\mathbf{0}$ eliminates the additional state variables. In this case, the reduced-order observer gives an estimate only of the variables that are not accessible (Ref. 12, pp. 276-279; for a more general case, *i.e.*, that in which $\mathbf{C}$ is a full-rank matrix with less rows than columns, see Ref. 12, pp. 284-286).

In particular, in this paper we will review the finite-state aerodynamic model of Refs. 8 and 9, and of the theory of the reduced-order observer.[12] In particular, we apply the formulation to a specific case and show that, if the finite-state aerodynamic model is stable, the design of the reduced-order observer of this state may be naturally given in terms of the finite-state aerodynamic model (Ref. 12, p. 227). Mastroddi and Morino are responsible for the theoretical formulation; Mastroddi, De Troia and Pecora for the numerical results.

Finite-State Aerodynamic Model

The basic model used and proposed in Morino *et al* [8] consists of approximating the aerodynamic matrix $\mathbf{E}(p)$ as

$$\begin{aligned} \mathbf{E}(p) &\simeq \hat{\mathbf{E}}(p) \\ &:= p^2\mathbf{E}_2 + p\mathbf{E}_1 + \mathbf{E}_0 + (p\mathbf{I} + \mathbf{G})^{-1}\mathbf{F}p \end{aligned} \tag{9}$$

where $\mathbf{G}$ and $\mathbf{F}$ are full square matrices which are independent of p. The aeroelastic system resulting from Eqs. 1, 4, and 9 is given by, in the time domain,

$$\begin{aligned} &\frac{U_\infty^2}{\ell^2}\ddot{\mathbf{q}} + \mathbf{\Omega}^2\mathbf{q} = q_D\left(\mathbf{E}_2\ddot{\mathbf{q}} + \mathbf{E}_1\dot{\mathbf{q}} + \mathbf{E}_0\mathbf{q} + \mathbf{r}\right) \\ &\dot{\mathbf{r}} + \mathbf{G}\mathbf{r} = \mathbf{F}\dot{\mathbf{q}} \end{aligned} \tag{10}$$

with $\mathbf{r}(0) = 0$ and where the overdot denotes differentiation with respect to $U_\infty t/\ell$. The matrices $\mathbf{E}_h$, $\mathbf{G}$, and $\mathbf{F}$ are obtained by a least-square approach which consists of setting

$$\varepsilon^2 = \int_0^\infty w(k)\,\mathrm{Tr}\left[\mathbf{Z}^*(ik)\mathbf{Z}(ik)\right]\,dk = \min \tag{11}$$

where $k = \Im mag(p)$ and

$$\mathbf{Z}(p) := (p\mathbf{I} + \mathbf{G})[p^2\mathbf{E}_2 + p\mathbf{E}_1 + \mathbf{E}_0 - \mathbf{E}(p)] + p\mathbf{F} \tag{12}$$

whereas $w(k)$ is a suitable weight function in the frequency range of interest (see Morino *et al* [8] for details). In addition, Tr denotes the trace of the matrix, and $\mathbf{Z}^*$ denotes the Hermitean adjunct of $\mathbf{Z}$ (complex conjugate of the transpose of $\mathbf{Z}$). Note that from Eq. 9, we have

$$\hat{\mathbf{E}}(p)\Big|_{p=0} = \mathbf{E}_0 \tag{13}$$

Accordingly, in the following $\mathbf{E}_0$ is considered as prescribed from the above equation (and not available for the minimization process). Thus, Eq. 12 may be rewritten as

$$\begin{aligned} \mathbf{Z}(p) &= p^3\mathbf{N}_3 + p^2\mathbf{N}_2 + p\mathbf{N}_1 + \mathbf{G}\mathbf{E}_0 \\ &\quad - (p\mathbf{I} + \mathbf{G})\,\mathbf{E}(p) \end{aligned} \tag{14}$$

where $\mathbf{N}_3 = \mathbf{E}_2$, $\mathbf{N}_2 = \mathbf{E}_1 + \mathbf{G}\mathbf{E}_2$, $\mathbf{N}_1 = \mathbf{E}_0 + \mathbf{G}\mathbf{E}_1 + \mathbf{F}$. The least-square minimization in Eq. 11 is performed with respect to $\mathbf{G}$, $\mathbf{N}_1$, $\mathbf{N}_2$, and $\mathbf{N}_3$. Note that the error function in Eq. 11 is a quadratic function of the elements of these matrices. Therefore, the least-square process yields a system of linear algebraic equation. Once $\mathbf{G}$ and $\mathbf{N}_k$ $(k = 1, 2, 3)$ have been obtained, the above expressions for $\mathbf{N}_3$, $\mathbf{N}_2$, $\mathbf{N}_1$, may be used sequentially to yield $\mathbf{E}_2$, $\mathbf{E}_1$, and $\mathbf{F}$, respectively (for higher-order formulations, see Refs. 8-11).

Formulation of a Reduced-Order Observer

Combining the Eqs. 3, 4, and 9, one obtains, in the time domain,

$$\dot{\mathbf{x}} = \mathbf{A}\mathbf{x} + \mathbf{b}\,u \tag{15}$$

where

$$\mathbf{x} := \left\{ \begin{matrix} \mathbf{q} \\ \dot{\mathbf{q}} \\ \mathbf{r} \end{matrix} \right\} \qquad \mathbf{b} := \left\{ \begin{matrix} \mathbf{0} \\ \mathbf{b}_2 \\ \mathbf{0} \end{matrix} \right\} \tag{16}$$

$$\mathbf{A} := \left[\begin{array}{c|c|c} \mathbf{0} & \mathbf{I} & \mathbf{0} \\ \hline \mathbf{P}(q_D\mathbf{E}_0 - \mathbf{K}) & q_D\mathbf{P}\mathbf{E}_1 & \mathbf{P} \\ \hline \mathbf{0} & \mathbf{F} & -\mathbf{G} \end{array} \right] \tag{17}$$

where $\mathbf{P} := (U_\infty^2\mathbf{M}/\ell^2 - q_D\mathbf{E}_2)^{-1}$, $\mathbf{b}_2 := \mathbf{P}\hat{\mathbf{b}}$, whereas $\mathbf{E}_i$ $(i = 0, 1, 2)$, $\mathbf{F}$, and $\mathbf{G}$ are the $(N+1) \times (N+1)$ aerodynamic matrices (see Eq. 10) which take into account also the degree of freedom relative to the control surface.

The standard description of the aeroservoelastic system is completed by the output relation, Eq. 6. In the following we assume that the output vector $\mathbf{y}$ is composed by the normal displacements δ_k and velocities v_k in $N+1$ suitable points of the wing where the sensors are locked:

$$\mathbf{y} := \{\delta_1, ..., \delta_{N+1}, v_1, ..., v_{N+1}\}^{\mathrm{T}} \tag{18}$$

Then, the output matrix is defined as

$$\mathbf{C} := \begin{bmatrix} \mathbf{\Phi} & \mathbf{0} & \mathbf{0} \\ \mathbf{0} & \mathbf{\Phi} & \mathbf{0} \end{bmatrix} = [\mathbf{C}_1|\mathbf{0}] \tag{19}$$

where $\mathbf{\Phi} := \phi_{n,k} \cdot \mathbf{n}_k$ is the square modal matrix the columns of which are the normal component of the $N+1$ modes used in the analysis (evaluated in the $N+1$ sensor locations). Here we assume that the location of the sensors is such as the matrix $\mathbf{\Phi}$ is non-singular. Then, in this special case, it is possible to group the state variables into two sets:[12] those that can be measured directly by the output vector $\mathbf{y}$,

$$\mathbf{x}_1 \equiv \left\{ \frac{\mathbf{q}}{\dot{\mathbf{q}}} \right\}^{\mathrm{T}} = \mathbf{C}_1^{-1}\mathbf{y} \tag{20}$$

and those that do not,

$$\mathbf{x}_2 \equiv \mathbf{r} \tag{21}$$

Accordingly, Eqs. 16, 20, and 21, Eqs. 15 and 6 may be written as

$$\dot{\mathbf{x}}_1 = \mathbf{A}_{11}\mathbf{x}_1 + \mathbf{A}_{12}\mathbf{x}_2 + \mathbf{b}_1 u \tag{22}$$

$$\dot{\mathbf{x}}_2 = \mathbf{A}_{21}\mathbf{x}_1 + \mathbf{A}_{22}\mathbf{x}_2 + \mathbf{b}_2 u \tag{23}$$

$$\mathbf{y} = \mathbf{C}_1\mathbf{x}_1 \tag{24}$$

with obvious definitions of all the matrices (in our case $\mathbf{b}_2 = \mathbf{0}$, see Eq. 10). If we were to use the full-state observer, we would obtain the estimate $\hat{\mathbf{x}} = \{\hat{\mathbf{x}}_1|\hat{\mathbf{x}}_2\}^{\mathrm{T}}$ of the state vector $\mathbf{x}$, from a system (full-state observer) given by (Ref. 12, p. 277)

$$\dot{\hat{\mathbf{x}}}_1 = \mathbf{A}_{11}\hat{\mathbf{x}}_1 + \mathbf{A}_{12}\hat{\mathbf{x}}_2 + \mathbf{b}_1 u + \mathbf{Q}_1(\mathbf{y} - \mathbf{C}_1\hat{\mathbf{x}}_1) \tag{25}$$

$$\dot{\hat{\mathbf{x}}}_2 = \mathbf{A}_{21}\hat{\mathbf{x}}_1 + \mathbf{A}_{22}\hat{\mathbf{x}}_2 + \mathbf{b}_2 u + \mathbf{Q}_2(\mathbf{y} - \mathbf{C}_1\hat{\mathbf{x}}_1) \tag{26}$$

where, the matrix $\mathbf{Q} = \left[\frac{\mathbf{Q}_1}{\mathbf{Q}_2} \right]$ should be designed in order to have stable eigenvalues for the matrix $\mathbf{A} - \mathbf{QC}$. In contrast, in the reduced-order observer formulation,[12] we choose $\hat{\mathbf{x}}_1 \equiv \mathbf{x}_1 = \mathbf{C}_1^{-1}\mathbf{y}$; then, Eq. 25 may be dropped, whereas Eq. 26 reduces to

$$\dot{\hat{\mathbf{x}}}_2 = \mathbf{A}_{22}\hat{\mathbf{x}}_2 + \mathbf{A}_{21}\mathbf{C}_1^{-1}\mathbf{y} + \mathbf{b}_2 u \tag{27}$$

The design of the controller, either by eigenvalues assignment or by optimal control, yields (see Eq. 7; note that, in the present case of single input, $\mathbf{K}$ is a row matrix denoted by $\mathbf{k}^{\mathrm{T}}$)

$$u = -\mathbf{k}^{\mathrm{T}}\hat{\mathbf{x}} = -[\mathbf{k}_1^{\mathrm{T}}|\mathbf{k}_2^{\mathrm{T}}] \left\{ \frac{\mathbf{x}_1}{\hat{\mathbf{x}}_2} \right\} \tag{28}$$

The resulting system is given by Eqs. 15, 27, and 28. The dynamics of the system is clearer if one introduces the observer error $\mathbf{e}_2 := \mathbf{x}_2 - \hat{\mathbf{x}}_2$; then Eqs. 15, 27, and 28 are replaced by[12]

$$\dot{\mathbf{x}} = (\mathbf{A} - \mathbf{bk}^{\mathrm{T}})\mathbf{x} + \mathbf{bk}_2^{\mathrm{T}}\mathbf{e}_2 \tag{29}$$

$$\dot{\mathbf{e}}_2 = \mathbf{A}_{22}\mathbf{e}_2 \tag{30}$$

which describe the closed-loop dynamics. From these equations we see that the dynamics of the error $\mathbf{e}_2$ (which goes to zero if $\mathbf{A}_{22} \equiv -\mathbf{G}$ is stable) is independent of $\mathbf{x}$ and produces a driving terms to the ideally-controlled system ($u = -\mathbf{k}^{\mathrm{T}}\mathbf{x}$ instead of $u = -\mathbf{k}^{\mathrm{T}}\hat{\mathbf{x}}$), *i.e.*, the system in absence of observer, as it would be obtained if the state vector is measurable). Consistently, as the characteristic equation of the overall system is

$$|p\mathbf{I} - (\mathbf{A} - \mathbf{bk}^{\mathrm{T}})| \; |p\mathbf{I} - \mathbf{A}_{22}| = 0 \tag{31}$$

In the case of stable aerodynamics this implies that the global closed loop system (observer plus regulator) has eigenvalues which are those of the ideally controlled closed-loop system plus those of the observer (*i.e.*, $\mathbf{A}_{22} \equiv -\mathbf{G}$).

Note that the system matrix $\mathbf{A}$ and, specifically, the submatrix $\mathbf{A}_{22}$, is a matrix over which the designer has no control: then, if there are no assurance on the stability $\mathbf{A}_{22}$, a more general system for the recostruction of $\hat{\mathbf{x}}_2$ is needed for which the reader is addressed in Ref. 12. However, in the case of sufficiently stable finite state aerodynamic model, the design of the reduced-order observer is clearly unnecessary as naturally given by Eq. 27 (for the case in which $\mathbf{A}_{22}$ is not sufficiently stable, see Ref. 12, pp. 278-279).

Numerical Results

In this Section some applications are presented. First, some aerodynamic and aeroelastic results are shown in order to show the high accuracy of the system. Indeed, the fundamental premise of the use of the estimator is that the model of the plant is sufficiently accurate. Then, we present the design of aeroservoelastic estimator-compensator for flutter suppression: in these applications the finite-state aerodynamic model is stable (*i.e.*, the eigenvalues of the matrix $\mathbf{A}_{22} \equiv -\mathbf{G}$ have negative real part).

All the aerodynamic and aeroelastic results shown are relative to the test case of the wind-tunnel-test wing-tail provided by ALENIA (see Fig. 1 for the geometry) at $M_\infty = 0$ (however the formulation is identically applicable to potential subsonic and supersonic flows). The terms of the 4×4 aerodynamic matrix of the above test case are shown in Figs. 2 and 3, Ref. 8: for all the 16 terms of the matrix, the agreement between the finite-state approximation and our aerodynamic data (markers) obtained by the unsteady subsonic panel method introduced by Morino,[15] is highly satisfactory (for discussion of other issues such as influence of the sampled data, higher-order models convergence and comparisons with other finite-state modeling, the reader is referred to Morino *et al*[8]).

Next, consider the aeroelastic applications. Figure 4 depicts the root locus of the three-mode system (with-

out the control): the experimental results obtained in the wind tunnel of the D.N.W. laboratory indicate that flutter occurred at $U_F = 103\ m/s$. With the present analysis the flutter speed has been evaluated to be $U_F = 98\ m/s$. Additional aeroelastic validations of the aerodynamic model based on the above finite-state aerodynamic are presented in Refs. 8-11, for 2D and 3D cases compared with experimental and numerical results. For instance, for the experimental case studied by Dogget, Rainey, and Morgan[16] (who, for $M_\infty = .913$, find $\hat{U}_F := U_F/b\omega_2 = 4.94$ and $k_F := \omega_F 2b/U_\infty = .122$), we obtain $\hat{U}_F := U_F/b\omega_2 = 5.19$ and $k_F := \omega_F 2b/U_\infty = .136$, in excellent agreement with the experimental results, better that those of Guruswamy and Goorjian[17] ($\hat{U}_F := U_F/b\omega_2 = 8.80$, $k_F := \omega_F 2b/U_\infty = .045$), obtained using a transonic finite-difference code.

Next, consider aeroservoelastic results. The configuration test used is the same as that discussed above, for Figs. 1-4.

The results are obtained using the classical linear-quadratic optimal control theory, Frieland[12] and Bryson[14] which is here summarized. Considering for the system given by Eq. 15, the linear control law given by Eq. 28 minimizes the performance index

$$J := \frac{1}{2}\int_0^{t_f} \left(\mathbf{x}^T\bar{\mathbf{Q}}\mathbf{x} + \mathbf{u}^T\bar{\mathbf{R}}\mathbf{u}\right) dt + \frac{1}{2}\mathbf{x}^T\bar{\mathbf{P}}\mathbf{x}\Big|_{t=t_f} \tag{32}$$

where t_f is the final time, $\bar{\mathbf{Q}}$ and $\bar{\mathbf{P}}$ are positive semi-definite, and $\bar{\mathbf{R}}$ is a positive definite. The optimal control matrix $\mathbf{K}_{\text{opt}}$ is given by

$$\mathbf{K}_{\text{opt}} = -\bar{\mathbf{R}}^{-1}\bar{\mathbf{B}}^T\mathbf{S} \tag{33}$$

where $\mathbf{S}$ is the definite positive solution of the stationary Riccati equation

$$\mathbf{S}\bar{\mathbf{B}}\bar{\mathbf{R}}^{-1}\mathbf{B}^T\mathbf{S} - \mathbf{S}\mathbf{A} - \mathbf{A}^T\mathbf{S} - \bar{\mathbf{Q}} = \mathbf{0} \tag{34}$$

For the above applications $\bar{\mathbf{Q}}_{ij} = 100\,\delta_{ij}$ and $\bar{\mathbf{R}}_{11} = 100$ where δ_{ij} is the dirac delta function and with the optimal control law evaluated at $U = 66\ m/s$ (matrices $\mathbf{A}$ and $\mathbf{B}$ are function of the flight speed U_∞). Figure 5 depicts the root locus of the controlled system with reduced-order observer. In this case the flutter speed has been increased to $U_F = 123\ m/s$; note that the eigenvalues of $\mathbf{A}_{22}$ ($\lambda_1 = -0.2210$, $\lambda_2 = -0.5074$, $\lambda_{3,4} = -1.1313 \pm i0.56894$) are the only contribution to the global stability given by the observer (see Eq. 31). They are not functions of U_∞ and therefore they do not move in the root locus (crosses). In Figures 6-9 the time histories (initial conditions $\mathbf{x}_0 = \{0.15, 0, 0, 0, 0, 0, 0, 0, 0, 0, 0, 0\}^T$) of the first four generalized degrees of freedom in an uncontrolled flutter condition ($U = 100m/s$) with control off and then on (when $q_1 > 0.2$). Two curves are presented. In the solid curve we examine the ideally controlled (no observer) case, in which the control law is applied as if the whole state space vector were known. The presence of the reduced-order observer is considered for the dashed curves which are obtained by assuming to have an observation error $\mathbf{e}_{2_0} = \{1, 1, 1, 1\}^T$ at the switch-on time (see Eqs. 29 and 30). This value of $\mathbf{e}_{2_0}$ is intentionally high in order to emphasize how small its influence is. The reason for difference is apparent if we examine the root locus (Fig. 5): the eigenvalues of $\mathbf{A}_{22}$ have small real part and therefore they are not sufficiently damped; in addition their imaginary part is small and this explains the lack of oscillatory behavior. Indeeed, the transient of $\mathbf{e}_2$ are shown in Fig. 10. As mentioned above, in this case, if a higher damping is desired one should use the more general theory for reduced-order observer, as presented for instance in Ref 12, pp. 278-279; this aspect is now under investigation.

Acknowledgement

This work was partially supported by the Agenzia Spaziale Italiana and by the Ministero dell'Università e della Ricerca Scientifica e Tecnologica. The authors wish to thank Prof. Salvatore Monaco of University of Rome "La Sapienza" for his valuable discussions on the issue of observability.

References

1. Jones, R. T., "The Unsteady Lift of a Wing of Finite Aspect Ratio," NACA 681, 1940,
2. Vepa, R., "On the Use of Padé Approximants to Represent Unsteady Aerodynamic Loads for Arbitrarily Small Motions of Wings," AIAA Paper 76-17, Jan. 1976.
3. Roger, K. L., "Airplane Math Modeling Methods for Active Control Design," AGARD-CP-228, Aug. 1977.
4. Edwards, J. W., Ashley, and H., Breakwell, J. V., "Unsteady Aerodynamic Modeling for Arbitrary Motions," *AIAA Journal,* Vol. 17, April 1979, pp. 365-374.
5. Edwards, J. W., "Application of Laplace Transform Methods to Airfoil Motion and Stability Calculations," AIAA Paper 79-0772, April 1979.
6. Karpel, M., "Design for the Active Flutter Suppression and Gust Alleviation Using State-Space Aeroelastic Modeling," *Journal of Aircraft,* Vol. 19, March 1982, pp. 221-227.
7. Venkatesan, C., and Friedmann, P. P., "New Approach to Finite-State Modeling of Unsteady Aerodynamics," *AIAA Journal,* Vol. 24, Dec. 1986, pp. 1889-1897.

8. Morino, L., Mastroddi, F., De Troia, R., and Pecora, M., "On the Modeling of Aeroservoelastic Problems," *Proceedings of the International Forum on Aeroelasticity and Structural Dynamics,* Strasbourg, France, May 1993, pp. 97-116.
9. Mastroddi, F., "Aeroservoelasticità: problematiche nonlineari," Tesi di Dottorato di Ricerca, Aerospace Department, Università degli Studi di Roma "La Sapienza", Rome, Italy, 1994.
10. Ghiringhelli, G. L., and Mantegazza, P., "Interpolation Extrapolation and Modeling of Unsteady Linear(ized) Aerodynamic Forces," *Proceedings of the International Forum on Aeroelasticity and Structural Dynamics,* Strasbourg, France, May 1993, pp. 207-221.
11. Morino, L., Mastroddi, F., De Troia, R., Ghiringhelli, G. L., Mantegazza, P., "Matrix Fraction Approach for Finite-State Aerodynamic Modeling," submitted to *AIAA Journal.*
12. Frieland, B., *Control System Design - An introduction to State-Space Methods,* McGraw-Hill, Inc., 1986.
13. Lu, P. J., Huang, L. J., "Optimal Control Law Synthesis for Flutter Suppression Using Active Acoustic Excitations," *Journal of Guidance, Control, and Dynamics,* Vol. 16, Jan.-Feb. 1993, pp. 124-131.
14. Bryson, A. E., Ho, Y., *Applied Optimal Control - Optimization, Estimation and Control,* Hemisphere, New York, NY, 1975.
15. Morino, L., "A General Theory of Unsteady Compressible Potential Aerodynamics," NASA CR-2464, Dec. 1974.
16. Doggett, R. V., Rainey, A. G., and Morgan, H. G., "An Experimental Investigation of Aerodynamic Effects of Airfoil Thickness on Transonic Flutter Characteristics," NASA TM X-79, 1959.
17. Guruswamy, P., Goorjian, P. M., "Comparisons Between Computations and Experimental Data in Unsteady Three-Dimensional Transonic Aerodynamics, Including Aeroelastic Applications," NASA TN 82-0690, 1982.
18. Kailath, T., *Linear Systems,* Prentice-Hall Information and System Science Series, Prentice-Hall, Inc., Englewood Cliffs, N.J., 1980.

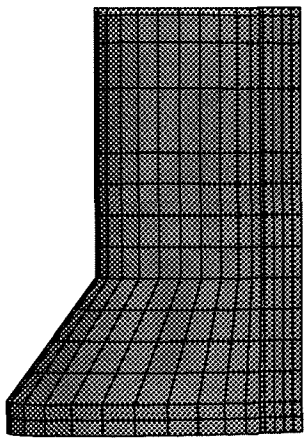

Figure 1: Geometry and aerodynamic mesh of the wind-tunnel-test wing-tail considered for the analysis: geometical and structural data provided by ALENIA.

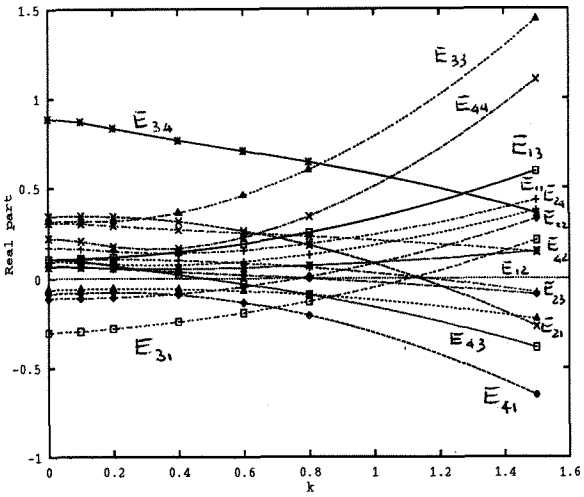

Figure 2: Real part *vs* reduced frequency of the 4×4 aerodynamic matrix (4 modes assumed) for the wind-tunnel-test wing-tail provided by ALENIA.

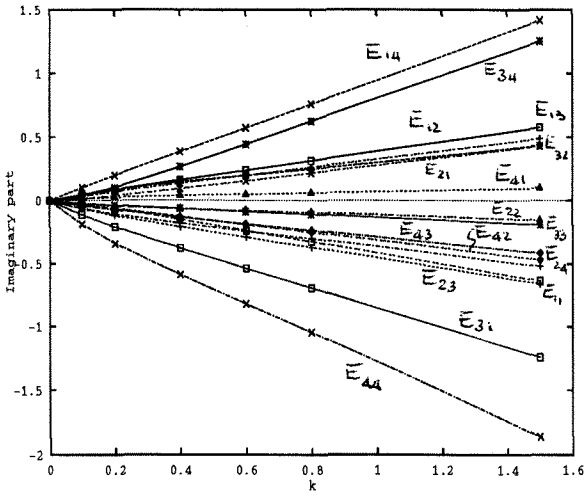

Figure 3: Imaginary part *vs* reduced frequency of the 4×4 (4 modes assumed) aerodynamic matrix for the wind-tunnel-test wing-tail provided by ALENIA.

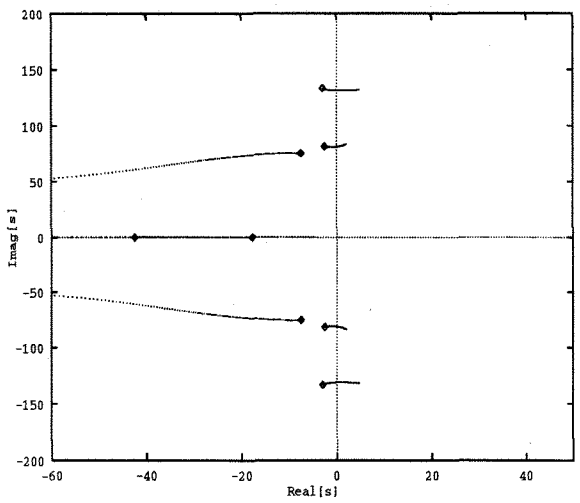

Figure 4: Root locus ($60m/s < U < 145m/s$) for the stability analysis of the wind-tunnel-test wing-tail ($M_\infty = 0$) without control ($U_F = 98m/s$).

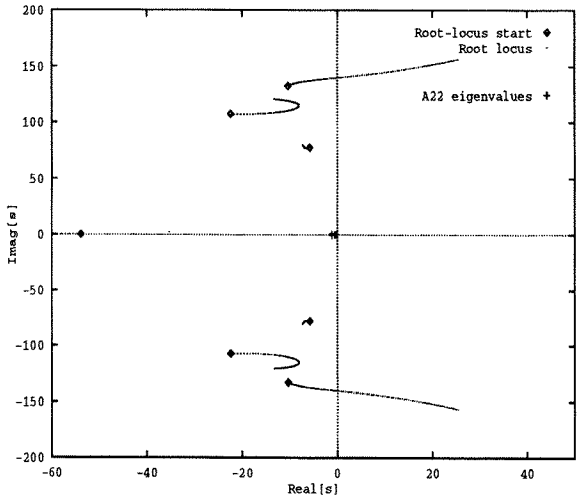

Figure 5: Root locus ($80m/s < U_\infty < 180m/s$) for the stability analysis of the wind-tunnel-test wing-tail ($M_\infty = 0$) with optimal control law evaluated at $U = 66m/s$ ($U_F = 123m/s$).

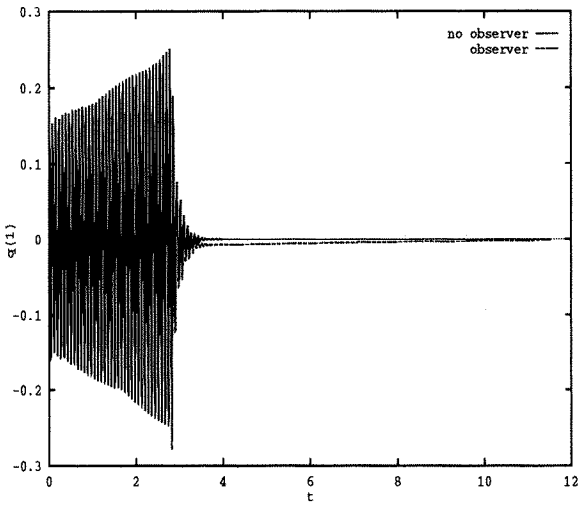

Figure 6: Time history of the first Lagrangean variable for the case of Fig. 1 in flutter condition: optimal control off and then on at $t = 2.8$.

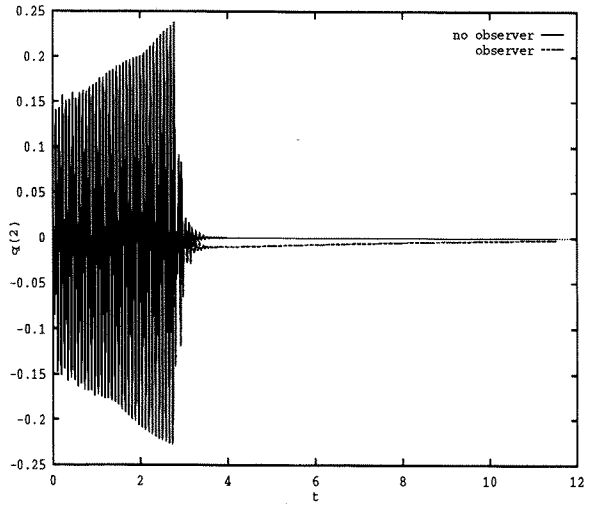

Figure 7: Time history of the second Lagrangean variable for the case of Fig. 1 in flutter condition: optimal control off and then on at $t = 2.8$.

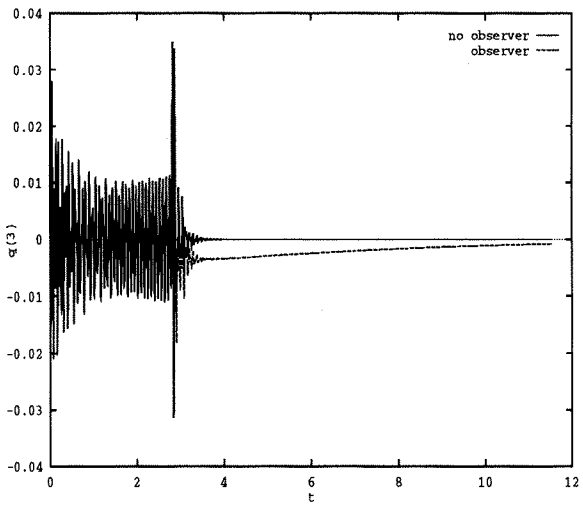

Figure 8: Time history of the third Lagrangean variable for the case of Fig. 1 in flutter condition: optimal control off and then on at $t = 2.8$.

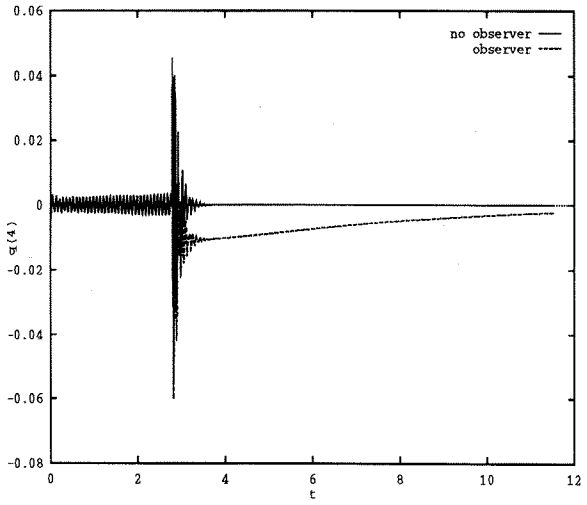

Figure 9: Time history of the fourth Lagrangean variable for the case of Fig. 1 in flutter condition: optimal control off and then on at $t = 2.8$.

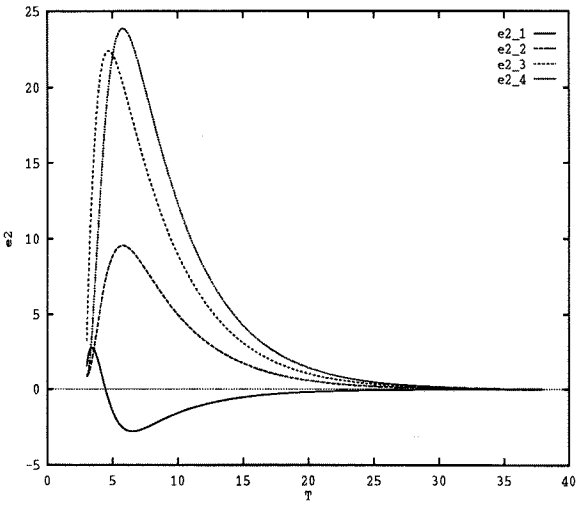

Figure 10: Time history of the observer error $\mathbf{e}_2$.